Dalton Transactions

Accepted Manuscript

This is an *Accepted Manuscript*, which has been through the Royal Society of Chemistry peer review process and has been accepted for publication.

Accepted Manuscripts are published online shortly after acceptance, before technical editing, formatting and proof reading. Using this free service, authors can make their results available to the community, in citable form, before we publish the edited article. We will replace this *Accepted Manuscript* with the edited and formatted *Advance Article* as soon as it is available.

You can find more information about *Accepted Manuscripts* in the Information for Authors.

ROYAL SOCIETY OF CHEMISTRY

www.rsc.org/dalton

Organotin(IV) based Anti-HCV drugs: Synthesis, Characterization and Biochemical Activity

Farooq Ali Shah[a], Shaista Sabir[b], Kaneez Fatima[c], Saqib Ali[a], Ishtiaq Qadri[d*], Corrado Rizzoli[e]

[a]Department of Chemistry, Quaid-i-Azam University, Islamabad 45320, Pakistan

[b]Research Complex, Department of Chemistry, Allama Iqbal Open University Islamabad Pakistan.

[c]IQ Institute of Infection and Immunity, Lahore, Pakistan

[d]Department of Medical Biotechnology, King Fahd Medical Research Center, King Abdul Aziz University, Jeddah, Saudi Arabia

[e]Department of Chemistry, University of Parma, Parma 43124, Italy

[*]Corresponding author address:

Prof. Ishtiaq Qadri, PhD
Head Medical Biotechnology
Head Liver Biology
Head Translational Research
King Fahd Medical Research Center
King Abdul Aziz University, Saudi Arabia.

Phone: +966 640 1000 Ext: 25218
Mobile: +966 53 516 8434
Fax: +966 6952 5321

Email:Ishtiaq80262@yahoo.com

Abstract

Three new organotin(IV) carboxylates (1–3) of 3,5-dimethylbenzoate, have been synthesized and characterized by elemental analysis, FT-IR, multinuclear NMR (^{1}H, ^{13}C and ^{119}Sn), mass spectrometry and single crystal X-ray structural analysis. Crystallographic data show that in compound **1** and **2,** the geometry at the central Sn atom is skew-trapezoidal bipyramidal while compound **3** displays distorted trigonal bipyramidal coordination geometry. In case of compound **1**and **2**, the asymmetric chelating mode of the carboxylate groups reflects in the unequal C-O bond distances, those observed for the O1 and O3 oxygen atoms being significantly longer than those found in the O2 and O4 atoms. In case of compound **3**, the carboxylate groups bridge asymmetrically adjacent tin atoms in an anti-syn mode generating polymeric zig zag chains running parallel to the crystallographic *c* axis.

The compounds were screened for the anti-HCV (hepatitis C Virus) potency by the Gaussia luciferase Assay using infected Huh 7.5 cells (human hepatocellular cell). Structure-activity relationship studies led to the identification of Dibutyltin(IV)bis(3,5-dimethylbenzoic acid) (compound **1**) as a potent HCV inhibitor, with Log IC_{50} values 0.69 nM in the cell-based assay. The compound **1** was further subjected to quantitative analysis using real-time PCR assays and viral RNA count vs drug concentration confirmed the Gaussia Luciferase Assay results. HCV RNA targeting mode of the compounds (1-3) were confirmed by compound-DNA interaction study. The compounds (1–3)-DNA interaction was investigated by UV–vis spectroscopy and viscometery. The hypochromic effect in spectroscopy evidenced intercalative mode of interaction with the binding affinity in 1 > 3 > 2 sequence.

Keywords: Organotin(IV) compounds, HCV, IC_{50}, luciferase assay, DNA, Binding energy constant.

Abstract

Three new organotin(IV) carboxylates (1–3) of 3,5-dimethylbenzoate, have been synthesized and characterized by elemental analysis, FT-IR, multinuclear NMR (^{1}H, ^{13}C and ^{119}Sn), mass spectrometry and single crystal X-ray structural analysis. Crystallographic data show that in compound **1** and **2,** the geometry at the central Sn atom is skew-trapezoidal bipyramidal while compound **3** displays distorted trigonal bipyramidal coordination geometry. In case of compound **1**and **2**, the asymmetric chelating mode of the carboxylate groups reflects in the unequal C-O bond distances, those observed for the O1 and O3 oxygen atoms being significantly longer than those found in the O2 and O4 atoms. In case of compound **3**, the carboxylate groups bridge asymmetrically adjacent tin atoms in an anti-syn mode generating polymeric zig zag chains running parallel to the crystallographic *c* axis.

The compounds were screened for the anti-HCV potency by the Gaussia luciferase Assay using infected Huh 7.5 cells (human hepatocellular cell). Structure-activity relationship studies led to the identification of Dibutyltin(IV)bis(3,5-dimethylbenzoic acid) (compound **1**) as a potent HCV inhibitor, with Log IC_{50} values 0.69 nM in the cell-based assay. The compound **1** was further subjected to quantitative analysis using real-time PCR assays and viral RNA count vs drug concentration confirmed the Gaussia Luciferase Assay results. HCV RNA targeting mode of the compounds (1-3) were confirmed by compound-DNA interaction study. The compounds (1–3)-DNA interaction was investigated by UV–vis spectroscopy and viscometery. The hypochromic effect in spectroscopy evidenced intercalative mode of interaction with the binding affinity in 1 > 3 > 2 sequence.

1. Introduction

Hepatitis C Virus (HCV) is a major health issue worldwide [1]. According to World Health Organization (WHO), more than 200 million carriers of the virus are present in the world [2]. Combination therapy with pegylated interferon (PEG-IFN-α) and ribavirin (RBV) has markedly improved the clinical outcome, but less than half of the proteins with chronic hepatitis C can be expected to respond favorably to the currently available agents [3]. Moreover, the present standard therapy (associated pegylated interferon and Ribavirin) [4,5] does not ensure a sustained virological response (SVR) in all genotypes [5]. The reappearance of circulating HCV-RNA after the end of treatment is very frequent and causes frustration in patients undergoing a full schedule of treatment with all related side effects. These problems raise the demand for the development of more efficacious, virus-specific, and better tolerated HCV inhibitors [6]. The advanced research revealed several targets in the HCV life cycle and its protein structural features for the development of potential HCV inhibitors [7-9].

The purpose of chronic hepatitis C therapy is the eradication of the infection and prevention of the cirrhosis development which may lead to hepatocellular carcinoma (HCC). Recently, organotin(IV) compounds have been found to be potent HCV inhibitors [10]. Organotin(IV) compounds have the ability to bind with RNA [11] and DNA [12] *via* electrostatic interaction of the $Sn(IV)^{+}$ moiety with the negatively charged oxygen of a phosphate group [11]. The single strand RNA provides greater accessibility to the Sn atom for interaction with nitrogenous bases as compared to double strand DNA and results in a more stable Sn–RNA adducts as compared to Sn–DNA compounds. The greater availability of the RNA basis for interaction with the Sn atom favors the interaction of the compound with viral RNA instead of human cell DNA in cell based assays. The Sn–RNA interaction quenches the RNA and ceases the production of RNA-

dependent RNA polymerase NS5B - responsible for the replication of the viral genome [13]. Spectroscopic and electrochemical methods have proven to be more reliable and frequently employed methods to study the interactions of metal compounds with DNA/RNA [14].

The development of HCV inhibitors requires continuous monitoring of HCV propagation in cell culture (HCVcc). Gaussia luciferase Assay [15] provides the best option for monitoring HCV propagation. Gaussia luciferase Assay has advantages over conventional methods for monitoring gene expression as this technique is more sensitive [16], requires few microliters of blood or urine, is time saving, does not involve any pretreatment and potential threat by exposing tissues to photon [17]. The Gaussia luciferase Assay, also helps to evaluate drug effects on cell proliferation, apoptosis, migration, and provides a higher throughput than time-consuming animal experiments [18,19].

In the search of developing potent and more specific anti- HCV agent, organotin(IV) derivatives of 3,5-dimethylbenzoic acid (HL) was prepared and characterized. In the formulation of a new drug, the proliferation of the drug across the cell membrane plays a significant role. In the present study, a small ligand with only polar group "carboxylic acid" is selected to formulate the drug of maximum permeability through cell membranes.

2. Experimental

3,5-Dimethylbenzoic acid and organotin(IV) chlorides were purchased from Aldrich Chemical (USA). Acetone, toluene, methanol, ethanol, n-hexane, and chloroform were obtained from Merck (Germany) and were purified before use [20]. RiboLock™ Ribonuclease inhibitor and RevertAid™ H Minus M-MuLV were purchased from Fermentas. Melting points of the synthesized compounds were recorded by the electrothermal melting point apparatus MP-D Mitamura Riken Kogyo (Japan) and are uncorrected. Elemental analysis was carried out using a

Leco CHNS- 932 analyzer. The IR spectra of the synthesized compounds were obtained using KBr pellets on a Bio-Rad Excaliber FT-IR spectrophotometer. Mass spectral data were collected on a Finnigan MAT-311A spectrometer. The ^{1}H and ^{13}C NMR spectra were recorded on a Bruker ARX 300 MHz-X Spectrometer at room temperature operating at 300 and 75.3 MHz, respectively. UV–visible spectrophotometric measurements were performed with a PerkinElmer Lambda 20 double-beam spectrophotometer, with the help of UV WinLab software (25 °C). Viscosity experiment was carried out using an Ubbelodhe Viscometer at 25 ± 1 ºC. "RoboGene® Hepatitis C virus Quantification Kit" (AJ Roboscreen GmbH, Leipzig Germany) was used for RNA extraction and reverse transcription. QIAquick PCR Purification Kit (Qiagen, USA) was used for the purification of RNA. The Jc1-FLAG2 (p7-nsGluc2A) RNA level inhibition was measured by a Real Time PCR instrument, MyiQ2TM System BIO-RAD Thermal Cycler, equipped with temperature probe (0.2 mL tube size).

2.1 Synthesis of organotin(IV) compounds

2.1.1 Synthesis of Dibutyltin(IV)bis(3′,5′-dimethylbenzoate) (1)

Compound **1** was synthesized by refluxing a mixture of Bu_2SnCl_2 (1.01 g, 3.35 mmol), 3′,5′-dimethylbenzoic acid (1 g, 6.7 mmol) and triethylamin (1.8 mL, 6.7 mmol) in dry toluene under refluxed for 8 h. The filtrate was concentrated to dryness at reduced pressure and the product was purified by recrystallization from chloroform and n-hexane (4:1v/v) mixture at room temperature. M.p. 131-132 °C: Anal.Calc. C 58.65; H 6.77; Found: C (58.74); H (6.72). IR (4000-200 cm^{-1}, KBr): 1555 ν (COasym) 1387 ν (COsym) 168 (Δν) 521 ν (Sn-C). ^{1}H NMR ($CDCl_3$, 300MHz) δ (ppm): 7.82 (s, 2H, 2/6); 7.24(s, 1H 4); 2.44(s, 6H 7/8); 0.92 (t, 7.2 terminal methyl protons of n-Butyl); 1.38-1.85 (m, 6H of first 3 carbons of Butyl). ^{13}C NMR ($CDCl_3$-d3, 75 MHz) δppm: 131(C1)**;** 127(C2/6); 138(C3/5); 127(C4); 40(C7/8); 167(C9); (29.37, 27.07,

26.67, 13.53, n-Butyl carbons). EI-MS, m/z (%): [SnL]269 (69), $[C_8H_9sn]^+$225 (28) , $[C_9H_9O_2]^+$149 (23), $[C_9H_9O]^+$133 (71), $[C_8H_9]^+$105 (100), $[C_6H_5]^+$77 (52), $[C_4H_9]^+$57 (41). ^{119}Sn NMR ($CDCl_3$): -170 ppm.

2.1.2 Synthesis of Dimethyltin(IV)bis(3′,5′-dimethylbenzoate) (2)

Compound **2** was synthesized in the same way as compound **1** by refluxing a mixture of Me_2SnCl_2 (0.73 g, 3.35 mmol), 3′,5′-dimethylbenzoic acid (1 g, 6.7 mmol) and triethylamin (1.8 mL, 6.7 mmol) in toluene. The filtrate was concentrated to dryness under reduced pressure and the product was purified by recrystallization from chloroform and n-hexane (4:1v/v) mixture at room temperature. M.p. 183-184 °C: Anal.Calc. C 58.97; H 3.69; Found: C (58.90); H (3.65). IR (4000-200 cm^{-1}, KBr): 1567 ν (COasym) 1425 ν (COsym) 142 (Δν) 515 ν (Sn-C). ^{1}H NMR ($CDCl_3$,300 MHz) δ (ppm): 7.58 (s, 2H, 2/6); 7.21(s, 1H 4); 2.50(s, 6H 7/8); 0.83 (t, 6H methyl protons) $^2J[^{119}Sn, ^1H]$ 78Hz. ^{13}C NMR ($CDCl_3$-d3, 75 MHz) δppm: 131(C1)**;** 127(C2/6)**;** 138(C3/5)**;** 127(C4)**;** 40(C7/8)**;** 167(C9); 29.2 ($^1J[^{119}Sn, ^{13}C]$ 622Hz methyl carbons). EI-MS, m/z (%): $[R_2SnCOOL]$433 (17), $[C_8H_9sn]^+$225 (23), $[RSn]^+$135 (15), $[C_9H_9O_2]^+$149 (18), $[C_9H_9O]^+$133 (69), $[C_8H_9]^+$105 (100), $[C_6H_5]^+$77 (53). ^{119}Sn NMR ($CDCl_3$): -135 ppm.

2.1.3 Synthesis of Trimethyltin(IV)(3′,5′-dimethylbenzoate) (3)

Compound **3** was synthesized by refluxing an equimolar amount of 3′,5′-dimethylbenzoic acid (1 g, 6.7 mmol), Me_3SnCl (1.33 g, 6.7 mmol) and triethylamin (0.93 mL, 6.7 mmol) in dry toluene. The filtrate was concentrated to dryness under reduced pressure and the product was purified by recrystallization from a chloroform methanol (4:1v/v) mixture at room temperature. M.p. 114-115 °C: Anal.Calc. C 45.85; H 5.73; Found: C (45.72); H (5.69). IR (4000-200 cm^{-1}, KBr): 1566 ν (COasym) 1424 ν (COsym) 142 (Δν) 506 ν (Sn-C). ^{1}H NMR ($CDCl_3$, 300MHz) δ (ppm): 7.70 (s, 2H, 2/6); 7.25(s, 1H 4); 2.37(s, 6H 7/8); 0.10(s, 9H $^2J[^{119/117}Sn, ^1H]$ 52, 58Hz

methyl protons). ^{13}C NMR ($CDCl_3$-d3, 75 MHz) δppm: 131(C1); 127(C2/6); 138(C3/5); 127(C4); 40(C7/8); 167(C9); -2.27 ($^1J[^{119}Sn, ^{13}C]$ 368Hz methyl carbons). EI-MS, m/z (%):[$R_2SnCOOL$]299 (32), $[C_8H_9Sn]^+$225 (24), $[R_2Sn]^+$150 (22), $[Sn]^+$120 (38), $[C_9H_9O_2]^+$149 (20), $[C_9H_9O]^+$133 (21), $[C_8H_9]^+$105 (100), $[C_6H_5]^+$77 (91). ^{119}Sn NMR ($CDCl_3$): 140 ppm.

2.2 Single-crystal X-ray analysis

Good quality single crystals of **1**, **2** and **3** were mounted on a Philips PW 1100, Bruker SMART 1000 CCD and Bruker APEX-II CCD diffractometer, respectively, equipped with graphite monochromatized Mo Kα radiation (λ = 0.71073 Å) fine-focus sealed tubes. For **2** and **3** intensity data were collected using ω scans while for **1** the $\omega/2\theta$ scan technique was used. Crystal data were collected using the Bruker SMART [21] and APEX-II [22] programs for **2** and **3** respectively, while the FEBO [23] system was used for **1**. Data refinement and reduction were performed using the FEBO system for compound **1**, the Bruker SAINT-Plus software [21] for **2** and the SAINT program [22] for **3**. Multi-scan absorption corrections were applied to the intensities of **2** and **3** using SADABS [21,22] while a psi-scan correction [24] was applied to the intensity data of **1**. The structures were solved by direct methods using the programs SHELXS-97 [25] or SIR97 [26], and refined with full-matrix least-squares based on F^2 using program SHELXL-97 [26]. All non-hydrogen atoms were refined anisotropically. Hydrogen atoms were placed geometrically and refined using a riding model approximation. In **1** the C21, C22, C25 and C26 carbon atoms of the n-butyl chains were found to be disordered over two orientations with a refined occupancy ratio of 0.701(4):0.299(4) for the major and minor components, respectively. During the refinement, the C-C bond distances and the C...C 1-3 separations involving the disordered atoms were restrained to be 1.54(1) and 2.53(1) Å respectively, and the

anisotropic displacement parameters of pairs of atoms in both components were set equal with the command EADP [26]. The molecular graphics and crystallographic illustrations were prepared using the ORTEP-3 for Windows [27] and SCHAKAL-99 [28] programs. All relevant crystallographic data and structure refinement parameters for **1**, **2** and **3** are summarized in Table 1. Selected bond lengths and angles for compounds **1**, **2** and **3** are listed in Tables 2, 3 and 4.

2.3 Anti-HCV Activity of organotin(IV) compounds by the Gaussia Luciferase Assay System

2.3.1 Virus stocks

The antiviral activity of compounds is evaluated by the Gaussia luciferase assay system [15]. In this assay, the fully-infectious HCVcc (HCV cell culture) viruses, Jc1FLAG2 (p7-nsGluc2A) was used to infect the Huh 7.5 cells. Jc1FLAG2 (p7-nsGluc2A) is a monocistronic reporter virus encoding the full-length infectious Jc1 genome with a second secreted Gaussia luciferase reporter. This is a highly sensitive HCVcc reporter virus expressing secreted Gaussia luciferase (Gluc), Jc1FLAG2 (p7-nsGluc2A). After inoculation, cultures were washed to remove Gluc carryover, and luciferase second secretion was monitored as an indicator of viral replication. Assay of luciferase activity in infected cell supernatants was used to monitor viral replication.

2.3.2 Cell culture

Huh7.5 cells were maintained in Dulbecco's modified Eagle's medium and incubated at 37 °C, 5% CO_2, and 100 % relative humidity. The compounds of 1 mg/mL strength in dimethyl sulfoxide were used. The cells were infected (with or without inhibitors), with Jc1-FLAG2 (p7-nsGluc2A) with MOI-0.1 (1E4 as median tissue culture infective dose [TCID50]/well) in the presence of the compound and the concentration of each compound used was between 1 nM to

1000 nM. Huh7.5 cells were incubated at 37 °C for 3 days, and luciferase activity measured using the EnduRen substrate (Promega). Infectious units (TCID50) were quantified by limiting dilution titration on naive Huh7.5 cells.

Maximum activity (100% of control) and background were derived from control wells containing DMSO alone or from uninfected wells, respectively. Add 100 µL of Lysis Buffer per well (Renilla Luciferase Assay Lysis Buffer diluted 5:1 in water) and shifting to a 96-Well plate. Store it on -80°C until it becomes ready to read on luminometer. 10 µL of each sample was added to the luciferase plate with Renilla Luciferase Assay, Buffer and Renilla substrate. The secreted Gaussia luciferase (Gluc) was measured on luminometer [29].

2.3.3 Quantitative Assay

The serum samples were collected from 56 patients suffering from HCV. All serum samples were negative for hepatitis B virus surface antigen (HBsAg) but positive for anti-hepatitis C virus antibody (anti-HCV ELISA). RNA was extracted from 140 µl of serum and it was eluted in 20 µL of hybridization solution containing 20U/ml of Ribonuclease inhibitor.

A mixture of 7 µL of extracted viral RNA, 1 µL of Reverse NS4A Primer and 3 µL of Diethylpyrocarbonate treated water were mixed gently using Microcentrifuge. Add mixture of 4 µL of 5X reaction buffer, 5 µL of RiboLock™ Ribonuclease Inhibitor (20 u/ µL) and 2 µL of Deoxynucleotide Triphosphates (10 mM) in it. The mixture is centrifuged and incubated at 37 °C for 5min. Add 1 µL of RevertAid™ H Minus M-MuLV in the mixture and incubate it at 42 °C for 60 min followed by heating at 70 °C for 10 min. The final mixture is centrifuged in the reaction tube and stored at – 20 °C for RT-PCR. For quantitative anti-HCV activity of the compound **1**, 1000, 667, 444, 198, 132, 26 and 0 nM of compound **1** was added. The RNA level

inhibition was measured by the Real Time PCR instrument. The strips were placed in the Real Time PCR instrument with ramping rate of 2.5 °C per search and the process was continued up to 3 hours for complete amplification of cellular RNA. The RT-PCR uses the amplified signal of product and measured as reaction progresses that are in "real time".

2.3.4 CT-DNA Interaction Study by UV-Visible Spectroscopy

CT-DNA (50 mg) was dissolved by stirring for overnight in double deionized water (pH = 7.0) and kept at 4 °C. The DNA solution in the buffer (20 mM Phosphate buffer "NaH_2PO_4-Na_2HPO_4" pH = 7.2) gave a ratio of 1.8 in UV absorbance at 260 and 280 nm (A_{260}/A_{280}), which indicates protein free DNA [30]. The DNA concentration was determined via absorption spectroscopy using the molar absorption coefficient of 6,600 M^{-1} cm^{-1} (260 nm) for the DNA [31] and was found to be 1.4×10^{-4} M. The solutions of the compounds of 0.2 mM strength were prepared in 80% ethanol. These stock solutions were used to form 9, 18, 27, 36, 45, 54 and 63 μM working solutions by dilution method. The UV absorption titrations were performed by keeping the concentration of the compound fixed while varying the DNA concentration. Equivalent solutions of DNA were added to the compound and reference solutions to eliminate the absorbance of DNA itself. Compound -DNA solutions were allowed to incubate for about 10 min at room temperature before measurements were made. The stability of the binding properties of the compounds studied towards DNA was examined by taking spectra after 24 and 48 h, and the same results were obtained.

2.3.5 Viscosity Measurements

For viscosity experiment, flow time was measured with a digital stopwatch and each sample was measured three times. Data were presented as $(\eta/\eta_o)^{1/3}$ vs. binding ratio (r) of [compound]/[DNA], where η and η_o are the relative viscosity of DNA in the presence of

compound and without compound. Viscosity values were calculated from the observed flow time of DNA-containing solutions corrected for the flow time (t_o) of 20 mM phosphate buffer solution (pH 7.2) alone. The viscosity for DNA in the presence and absence of the compound was calculated from the following equations [32];

$$\eta_o = t - t_o$$

and

$$\eta = \frac{t - t_o}{t_o}$$

3. Results and Discussion

3,5-Dimethylbenzoic acid (HL), triethylamine and diorganotin(IV) chlorides solution (2:1 molar ratios)/ triorganotin(IV) chloride (1:1 molar ratio) were mixed with anhydrous toluene (100 mL) and the reaction mixture was refluxed for 8h. Triethylamine hydrochloride was removed by filtration and the synthesized organotin(IV) derivatives were obtained in vacuum by removing solvents. The general procedures for the synthesis of organotin(IV) compounds **1**, **2** and **3** are shown in scheme 1.

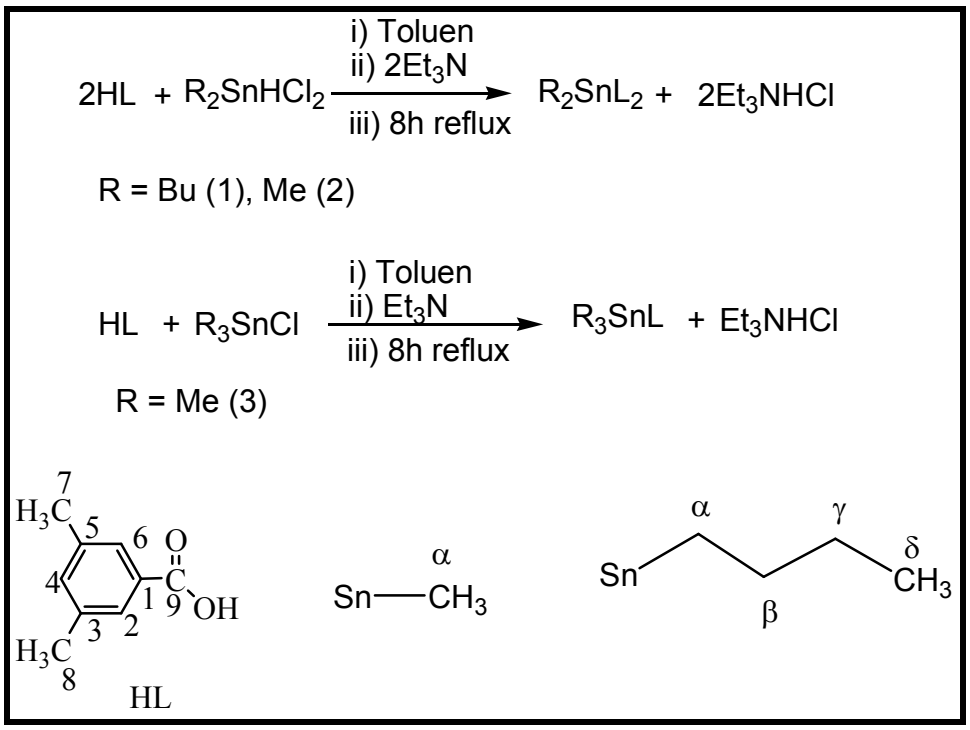

Scheme 1. General procedures for the synthesis of organotin(IV) compounds

3.1 X-ray crystallography

The molecular structure of compound **1**, **2** and **3** is shown in Fig. 1A, 1B and 1C respectively. In compound **1** and **2**, the carboxylate group COO^- of the ligands is bonded in an anisobidentate mode with two shorter bonds (Sn1-O1 and Sn1-O3, mean values 2.127(7) Å) and two longer bonds (Sn1-O2 and Sn1-O4, mean value 2.507(18) Å) as reported in Table 2 and 3. The geometry at the central Sn atom is skew-trapezoidal bipyramidal where the equatorial plane is defined by four oxygen atoms of the two chelating carboxylate ligands and the apical positions are occupied by the carbon atoms of two n-butyl (in **1**) or methyl (in **2**) groups. The longer Sn-O distances are remarkably shorter than the sum of the van der Waal's radii (3.68 Å) [33] in both cases. The dialkyltin fragments are arched along the longed edge of the equatorial trapezoid defined by the chelating atoms, the C-Sn-C angles

(148.50(16) and 148.67(11)° for compound**1** and **2**, respectively) falling in the range (122.6-156.9°) observed for a skew-trapezoidal bipyramidal geometry [34,35].

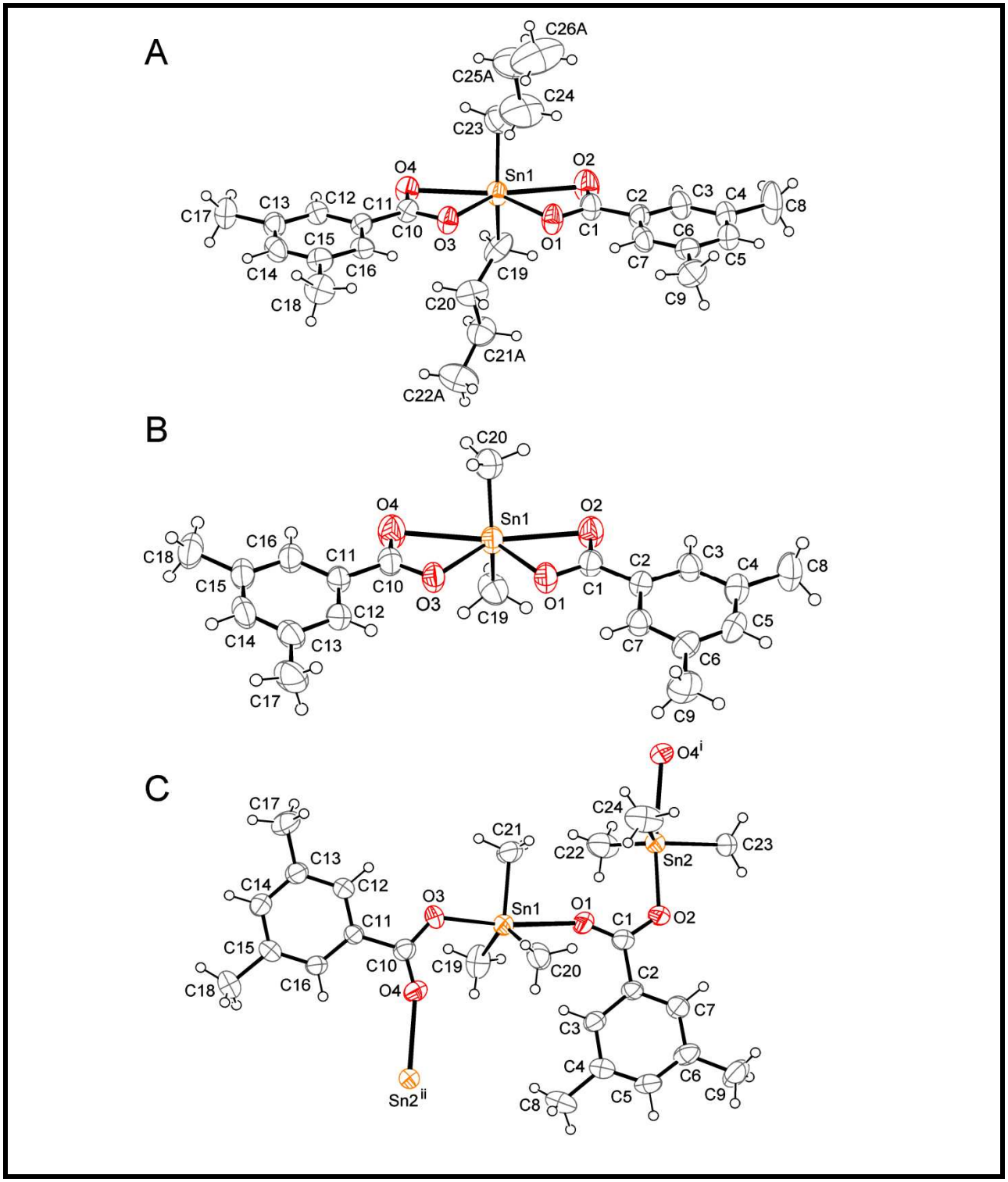

Fig. 1. ORTEP drawings of the asymmetric units of (A) compound 1, (B) compound 2 and (C) compound 3 with displacement ellipsoids drawn at the 50% probability level. In (A) only the

major components of the disordered n-butyl groups are shown. Symmetry codes for (C): (i) x, 1/2-y, -1/2+z; (ii) x, 1/2-y, 1/2-z.

The asymmetric chelating mode of the carboxylate groups reflects also in the unequal C-O bond distances, those observed for the O1 and O3 oxygen atoms (mean value 1.287 (3) Å) being significantly longer than those found in the O2 and O4 atoms (mean value 1.244(3) Å) involved in the longer Sn-O interactions.

For both compounds **1** and **2** π...π stacking interactions are effective in stabilizing the crystal structure. In **1**, centrosymmetrically related molecules are linked by pairs of π...π interactions (centroid-to-centroid distance 3.765(2) Å) into dimers, which are further connected by π...π contacts (centroid-to-centroid distance 3.750(2) Å) to form ribbons parallel to the (110) direction (Fig. 2A) whereas in **2** molecules are linked by π...π interactions (centroid-to-centroid distance 3.8608(15) Å) into chains extending along the (100) direction (Fig. 2B).

The asymmetric unit of compound **3** consists of two independent trimethyltin groups and two carboxylate ligands. Each metal atom displays a distorted trigonal bipyramidal coordination geometry, with the methyl carbon atoms forming the equatorial plane and the oxygen atoms of different carboxylate groups occupying the apical positions. The Sn-O bond lengths are remarkably different (Table 4) and in agreement with those reported in the literature for triorganotin(IV) carboxylates [36,37]. The distortion of the coordination polyhedra may be inferred by the deviation from the ideal geometry of the O-Sn-O (171.94(14) and 172.61(13)°) and C-Sn-C angles (115.8(3)-123.9(3)°). The carboxylate groups bridge asymmetrically adjacent tin atoms in an anti-syn mode generating polymeric zig zag chains running parallel to the crystallographic *c* axis (Fig. 2C). The polymeric bridging behavior is comparable with that observed for related compounds [33]. In the crystal structure (Fig. 2D), the polymeric chains are

linked into a three-dimensional network by by π...π stacking interactions (centroid-to-centroid distance 3.708(3) Å).

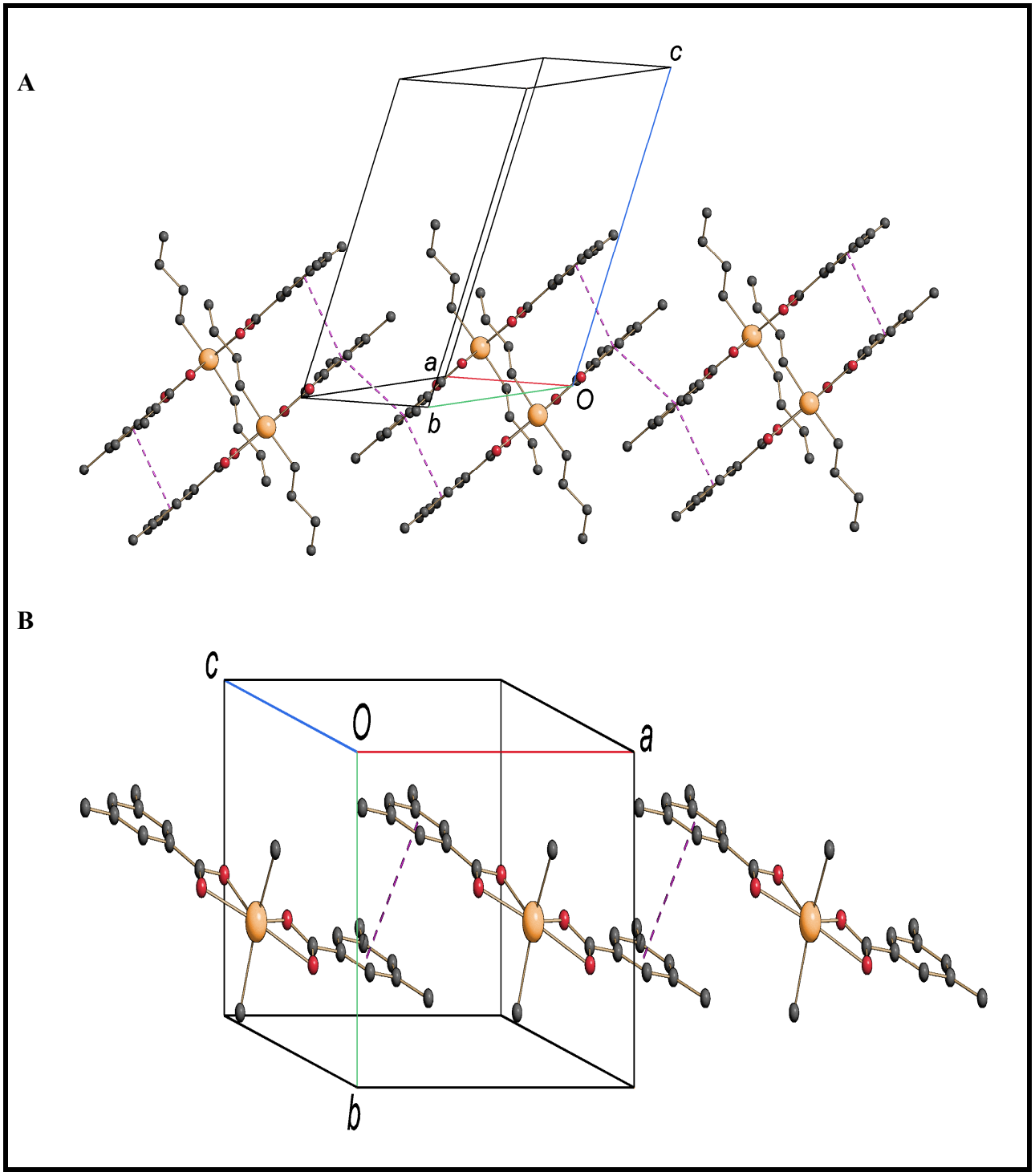

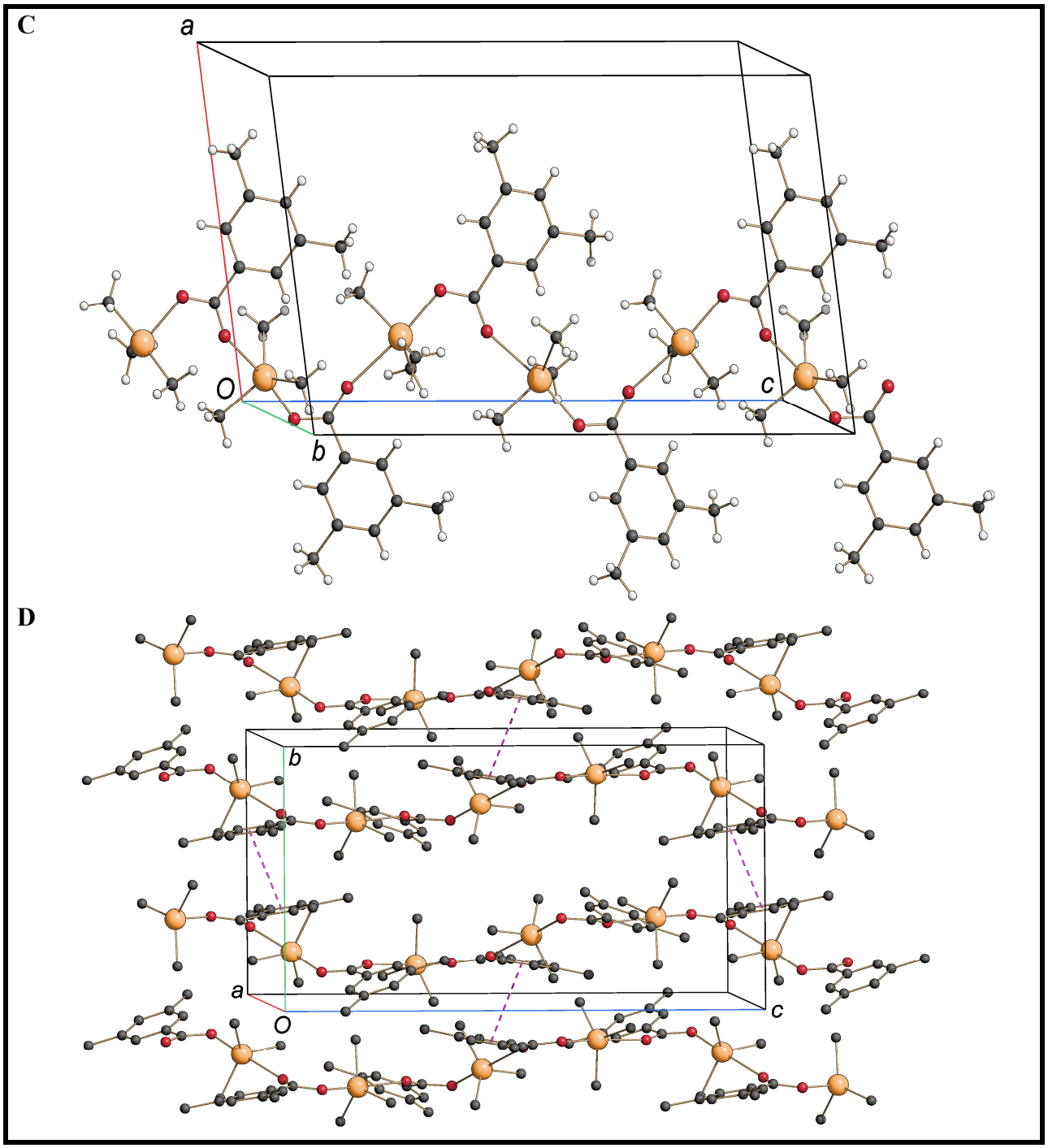

Fig. 2 (A). Partial crystal packing of 1 showing the formation of a molecular ribbon parallel to the (110) direction through π...π stacking interactions (dashed lines) while Hydrogen atoms are omitted for clarity. Only the major components of the disordered n-butyl groups are shown. (B). Partial crystal packing of 2, showing the formation of a molecular chain parallel to the *a* axis through π...π stacking interactions (dashed lines). Hydrogen atoms are omitted for clarity. (C). The polymeric chain of 3 extending along the *c* axis. (D). Crystal packing of 3 showing chains connected by π...π stacking interactions (dashed lines) into a three-dimensional network. Hydrogen atoms are omitted for clarity.

Table 1: Crystal data and structure refinement parameters for compounds 1, 2 and 3

	1	**2**	**3**
Emp. formula	$C_{26}H_{36}O_4Sn$	$C_{20}H_{24}O_4Sn$	$C_{24}H_{36}O_4Sn_2$
Formula weight	531.24	447.08	625.91
Crystal system	Triclinic	monoclinic	Monoclinic
Space group	*P*-1	$P2_1/c$	$P2_1/c$
a (Å)	9.566(3)	11.540(4)	12.041(3)
b (Å)	11.892(5)	7.298(2)	11.466(3)
c (Å)	13.438(5)	24.778(8)	20.435(5)
α (◦)	104.257(6)	90	90
β (◦)	99.468(6)	102.918(5)	99.367(4)
γ (◦)	109.702(8)	90	90
V ($Å^3$)	1342.6(9)	2034.0(11)	2783.7(12)
Z	2	4	4
Crystal size (mm)	0.21x0.18x0.06	0.22x 0.16x 0.07	0.18 x 0.10 x 0.07
Crystal habit	Plate	plate	Block
T (K)	295(2)	295(2)	294(2)
μ (mm^{-1})	0.977	1.275	1.818
λ(MoK_α) (Å)	0.71073	0.71073	0.71073
Total reflections	7836	23318	25358
Independent reflections	7823	4660	5023
Final R indices [I>2σ (I)]	R1 = 0.0423 wR2 =0.1058	R1 = 0.0267 wR2 =0.0678	R1 = 0.0335 wR2 =0.0666
R indices (all data)	R1 = 0.0618 wR2 =0.1126	R1=0.0312 wR2 =0.0710	R1 = 0.0876 wR2 =0.0817
Goodness-of-fit	0.970	1.097	0.938
θ range for data collections (◦)	3.19-30.00	1.69-27.52	1.71- 25.26
Data/restraints/parameters	7823/18/297	4660/0/232	5023/0/ 281

Table 2: Selected bond lengths (Å) and bond angles (˚) for 1

Sn1-O1	2.141(2)	Sn1-C23	2.127(4)
Sn1-O2	2.509(3)	O1-C1	1.289(4)
Sn1-O3	2.141(2)	O2-C1	1.251(4)
Sn1-O4	2.480(2)	O3-C10	1.274(4)
Sn1-C19	2.105(4)	O4-C10	1.254(3)
O1-Sn1-O2	55.75(9)	O2-Sn1-C23	86.78(14)
O1-Sn1-O3	84.63(9)	O3-Sn1-O4	55.81(8)
O1-Sn1-O4	140.43(8)	O3-Sn1-C19	103.51(13)
O1-Sn1-C19	99.47(13)	O3-Sn1-C23	102.01(14)
O1-Sn1-C23	101.01(14)	O4-Sn1-C19	89.77(13)
O2-Sn1-O3	140.38(9)	O4-Sn1-C23	89.49(13)
O2-Sn1-O4	163.80(8)	C19-Sn1-C23	148.50(16)
O2-Sn1-C19	85.25(14)		

Table 3: Selected bond lengths (Å) and bond angles (˚) for 2

Sn1-O1	2.1353(15)	Sn1-C20	2.095(3)
Sn1-O2	2.4819(17)	O1-C1	1.287(2)
Sn1-O3	2.1120(17)	O2-C1	1.245(2)
Sn1-O4	2.5483(18)	O3-C10	1.292(3)
Sn1-C19	2.095(3)	O4-C10	1.237(3)
O1-Sn1-O2	55.82(5)	O2-Sn1-C20	89.31(9)
O1-Sn1-O3	83.32(6)	O3-Sn1-O4	55.16(6)
O1-Sn1-O4	138.48(5)	O3-Sn1-C19	99.94(9)
O1-Sn1-C19	102.35(10)	O3-Sn1-C20	100.97(9)
O1-Sn1-C20	103.03(10)	O4-Sn1-C19	87.07(9)
O2-Sn1-O3	139.15(6)	O4-Sn1-C20	86.01(9)
O2-Sn1-O4	165.68(5)	C19-Sn1-C20	148.67(11)
O2-Sn1-C19	89.95(9)		

Table 4: Selected bond lengths (Å) and bond angles (˚) for 3

Sn1-O1	2.517(4)	Sn2-O2	2.130(3)
Sn1-O3	2.134(4)	Sn2-O4^{i}	2.607(4)
Sn1-C19	2.107(7)	Sn2-C22	2.094(6)
Sn1-C20	2.096(6)	Sn2-C23	2.106(6)
Sn1-C21	2.100(6)	Sn2-C24	2.075(6)
O1-C1	1.229(6)	O3-C10	1.278(6)
O2-C1	1.280(6)	O4-C10	1.231(6)
O1-Sn1-O3	171.94(14)	O2-Sn2- O4^{i}	172.61(13)
O1-Sn1-C19	87.1(2)	O2-Sn2-C22	98.5(2)
O1-Sn1-C20	86.6(2)	O2-Sn2-C23	89.52(19)
O1-Sn1-C21	82.42(19)	O2-Sn2-C24	98.1(2)
O3-Sn1-C19	93.8(2)	O4^{i} -Sn2-C22	88.0(2)
O3-Sn1-C20	99.4(2)	O4^{i} -Sn2-C23	84.53(19)
O3-Sn1-C21	90.1(2)	O4^{i} -Sn2-C24	80.8(2)
C19-Sn1-C20	123.9(3)	C22-Sn2-C23	115.8(3)
C19-Sn1-C21	117.5(3)	C22-Sn2-C24	124.4(3)
C20-Sn1-C21	116.7(3)	C23-Sn2-C24	116.9(3)

3.2 NMR

The ^{1}H and ^{13}C spectra were recorded in deutrated chloroform and the data of alkyl-tin species, chemical shift values are deducible from the multiplicity pattern and resonance intensities. The integration values obtained from the resulting spectra are in good agreement with the proposed structures. In the ^{1}H NMR spectra of the compounds, the complete absence of acidic proton signals suggests the deprotonation of acid and coordination mode to the tin through the oxygen atom of the ligand [38]. ^{n}J(Sn, H) couplings were not observed for the compound **1** due to the complex nature of the n-Bu group protons. The ^{1}H NMR spectrum of **3** showed a singlet for

CH_3–Sn, having a $^2J(^{119/117}Sn–^1H)$ value (52 and 58 Hz) suggesting a pentacoordinated structure while for compound **2**, $^2J(^{119}Sn–^1H)$ value is found 78 Hz which confirmed the octahedral geometry around tin [38].

The ^{13}C NMR spectra of the compound support the ^1H NMR data. In ^{13}C NMR, the Me and n-Bu groups attached to Sn atom signals are found in expected region. The shift is an outcome of an electron density transfer from the ligand to the tin atom. The coupling constants $^nJ(^{119}Sn–^{13}C)$ is one of the important parameters for the structure elucidation of organotin(IV) compounds. The ^1J $(^{119}Sn\text{-}^{13}C)$ coupling constants for the compound **3** shows the pentacoordination number around the tin suggesting trigonal-bipyramidal geometry [38] while $^1J(^{119}Sn, ^{13}C)$ value for compound 2 suggested octahedral geometry around the tin atom.

The ^{119}Sn NMR spectra of the compounds are in accordance with proposed one. ^{119}Sn chemical shift for compound **1** and **2** are similar as for five or six coordinated environment around the tin atom,while for compound **3** is similar as for four coordinated environment around the tin atom and consistency with literature values [38].

3.3 Anti-HCV Study

3.3.1 Gaussia Luciferase Assay

The Gaussia Luciferase Assay System was used to study the anti-HCV activity of the organotin(IV) compounds and dose vs response curve are plotted in 2A. In this assay Jc1FLAG2 (p7-nsGluc2A) [39] was used to infect the Huh 7.5 cells. The $logIC_{50}$ of the tested compounds are summarized in the Table 5 and plotted in Fig. 3B.

The dose-response curve in Fig. 3A shows that the viral inhibition depends upon the coordination number of the tin atom, nature and structure of the compound. Among the tested organotin(IV) carboxylates, the n-butyltin(IV) derivative was found more potent against HCV

than the methyl derivatives due to its optimal balance among cytotoxicity, solubility, and lypophilicity [40].

In organotin(IV) compounds, the role of the ligand and the symmetry of molecules in solution is important in defining the activity of the compound as ligand in a complex is responsible for the transportation of the organotin(IV) species to the site of the action. Previously, we have been working on determining the importance of ligands and substitution on these ligands in anti-HCV activity of the compounds [41]. Optimization of ligand suggests the use of the ligand with the least numbers of polar groups for improvement of activity. In the present case, a symmetrical and small size legend with carboxylate as the only polar group was selected. The small size of the ligand enhanced the activity of the compounds by facilitating an increased cellular uptake of these compounds and the approach of the molecules to the binding site in living systems.

Table 5. Gaussia Luciferase Assay and DNA-organotin(IV) interaction parameters

Comp	Ligand	Gaussia Luciferase Assay		Compounds-DNA Interaction Parameters by Spectroscopy	
		R	Log IC_{50} (nM)	K/M^{-1}	$-\Delta G/kJmol^{-1}$
1	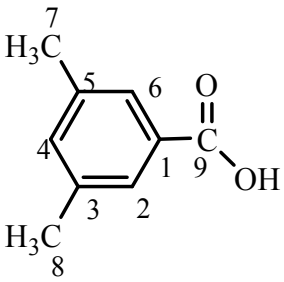	2Bu	0.69	4.35×10^4	26.5
2		2Me	3.20	1.04×10^4	22.9
3		3Me	1.34	1.34×10^4	23.5
4	Telaprevir		2.4		

Organotin(V) moieties are selected for this study due to their RNA binding capabilities. The targeting viral RNA with drug of novel structure in HCV treatment has advantages over targeting

proteins as the appearance of drug resistance by point mutations in an RNA motif is slow and the resistance developing capability can be easily overcome.

Among the tested organotin(IV) compounds, compound **1** shows the highest anti-HCV activity with a logIC_{50} value of 0.69. The dibutyltin(IV) moiety was replaced with the dimethyltin(IV) moiety to achieve a more simple and small size molecule, but the butyl group replacement reduced the anti-HCV activity of compound **2** by 4.64 times. The decrease in potency of compound **2** (3.20) may be attributed to the lowered lipophilicity of the resultant compound. The organotin(IV) moiety was further optimized by replacing the dimethyltin(IV) moiety with the trimethyltin(IV) moiety. This replacement provided compound **3** which showed an activity increased by a factor 2.4 with respect to compound **2**. In triorganotin(IV) moieties, five-membered stereochemistry around the thin metal make, it is more easily available to interact with biological systems through the unoccupied sixth position [42]. Compound **1** showed a doubled potency against HCV as compared to compound **3**, which can be attributed to its higher lipophilicity.

A

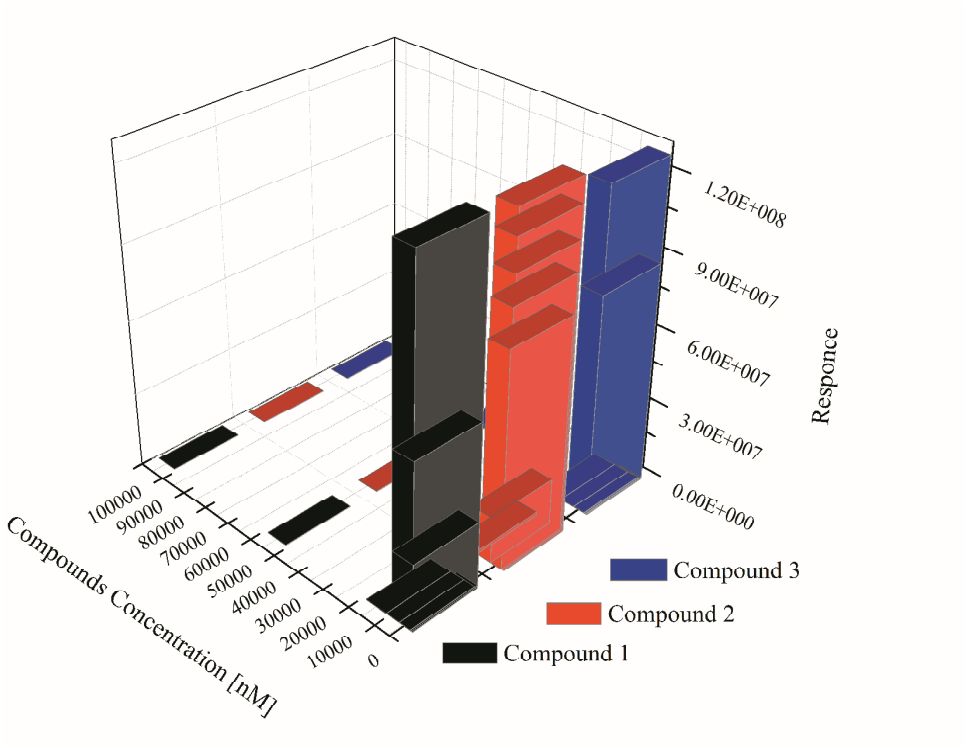

B

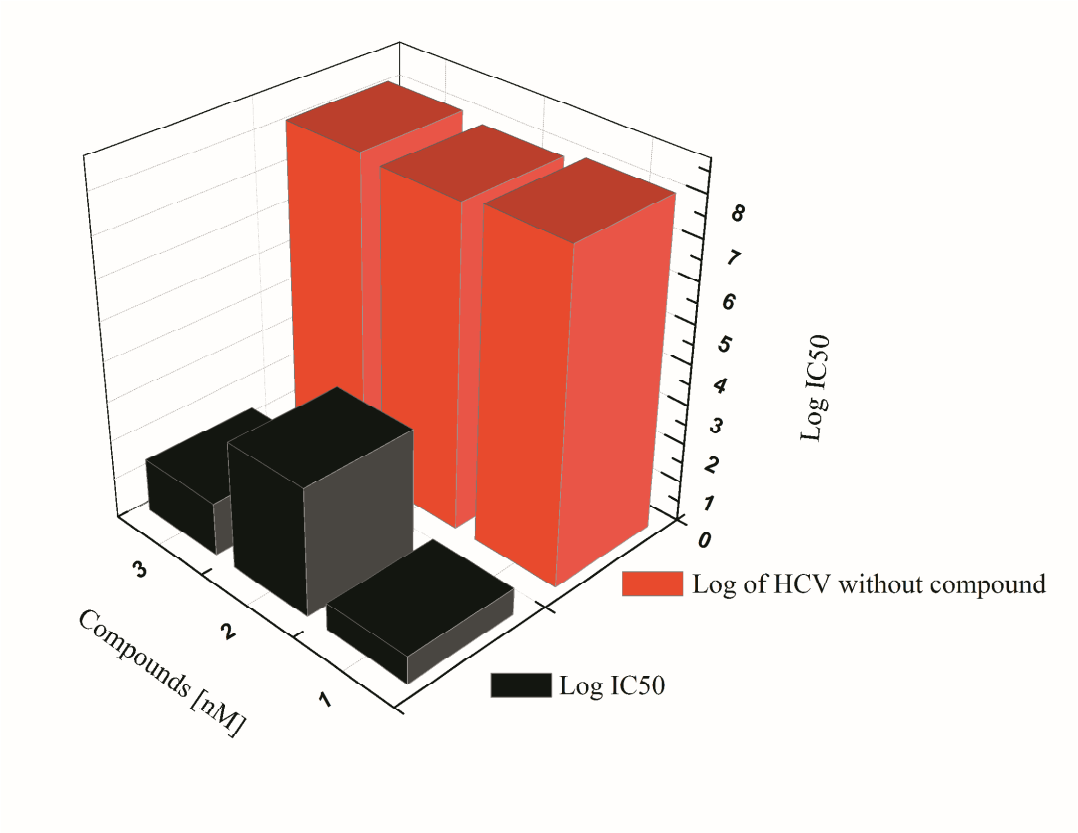

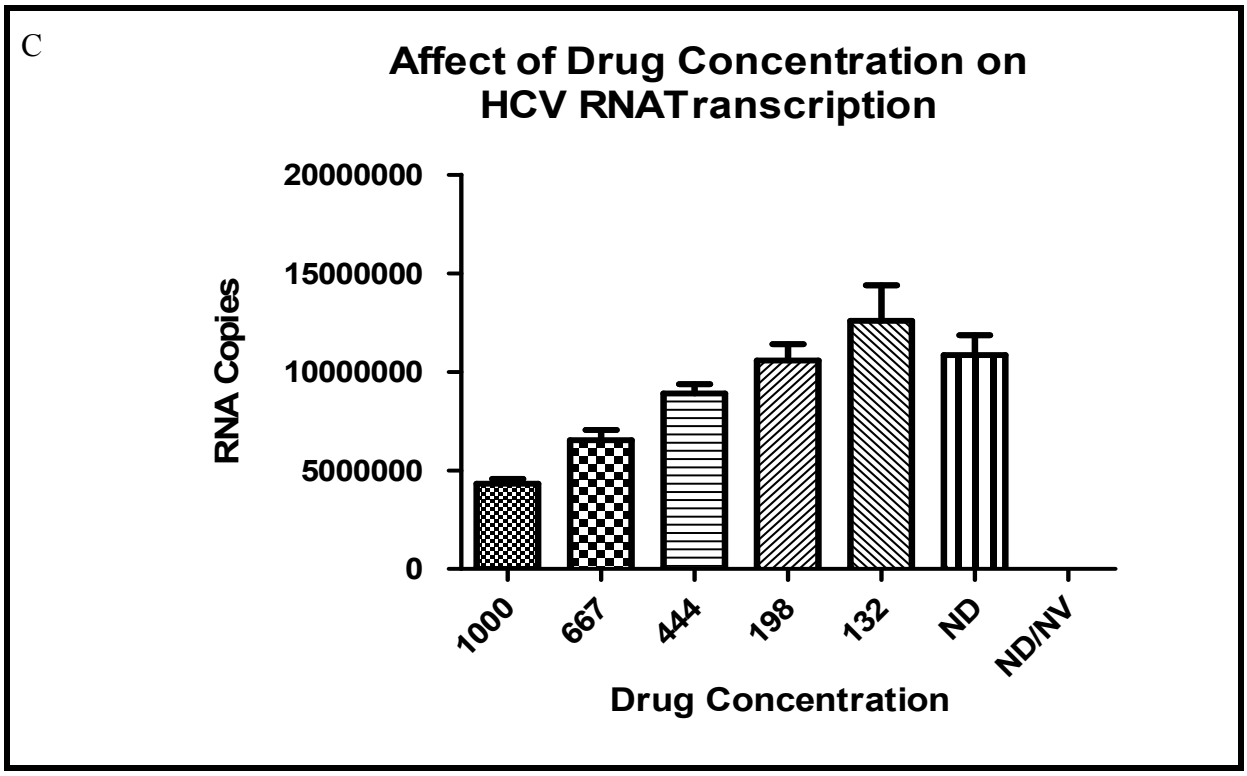

Fig.3. (A) Dose Vs Response curve for Compounds 1, 2 and 3 obtain from Gaussia Luciferase Assay System (B) LogIC50 of compounds 1, 2 and 3 (C) Dose response curve for compound1 from the Real Time PCR instrument

3.3.2 Quantitative Analysis of compound 1

On the basis of Gaussia Luciferase Assay results, compound **1** was selected for quantitative analysis by quantitative Real-Time PCR. Initially, the minimum and maximum concentrations (1000 nM and 10 nM of the compound **1**) were used for quantitative analysis to measure viral titers of compound**1** with Jc1FLAG-2. Samples were run through PCR to evaluate the effect of compound **1** on HCV RNA. The quantitative Real-Time PCR data are plotted in Fig. 3C as RNA Vs drug concentrations. The RNA Vs drug concentrations authenticated the decrease in viral replication by compound **1**. Compound **1** showed a gradual response between the effective concentrations and inhibitory activity (Fig. 3C). The RNA Vs drug concentrations showed that compound **1** is effective even at low concentration and the inhibition of HCV was steady with time.

Table 6. IC_{50} for compound1 by QRT-PCR

IC_{50} (nM)	Span	R^2
3.245±0.5668	40862	0.9531

Different statistical tools were used for determination of the effective drug concentrations using the QRT-PCR data. The statistical analysis suggested the IC_{50} value 3.24 nM with standard error of 0.5 (Table 6). This inhibition concentration is consistent with a previously determined IC_{50} value from Gaussia Luciferase Assay for compound **1**.

The cytotoxic effects of compound **1** at different concentrations show that the number of cells was greatly reduced by compound **1,** whereas the numbers of cells were intact in the controls of ND/NV ($p < 0.05$). Total cell counts were determined by the Trypan blue exclusion method using a hemocytometer. The effect of 1000nM concentration of compound **1** after 24 and 48h of incubation (Table 7), suggest it a future candidate for lowering viral replication.

Table 7. Cell viability Assay for compound 1

Sample	**0 Hrs***	**24 Hrs***	**48 Hrs***
ND/NV	1000,000	1200,000	1500,000
Compound **1**	1000,000	550,000	110,000
No Drug	1000,000	1100,000	1400,000

**The numbers shown above are mean of three experiments. Variation among the results were less than 6%.*

3.4 Compound -DNA interaction study

3.4.1 UV-Vis absorption study of compound-DNA interaction

Thermodynamic parameters of the organotin (IV) compounds - DNA interaction was determined by UV-Vis spectroscopy, which helped in determining the mode of interaction and binding

strength. The effect of varying concentrations of DNA (9-63 μM) on the electronic absorption spectra of 0.2 mM of **1, 2 and 3** is shown in Fig. 4A-C. The absorption spectra of **1**, **2** and **3** recorded 24**,** 21 and 27% decrease in peak intensities accompanied with slight blue shift (1~2 nm) by the addition of 63 mM DNA. These spectral characteristics are indicative of drug binding to DNA, which results in conformational and structural change of DNA [43,44]. The hypochromism effects observed here is attributed to the intercalation of these compounds into the DNA base pairs. In the intercalation binding mode, the π* orbital of the binding ligand couple with the π orbital of DNA base pairs. The coupling π* orbital is partially filled, which decreases the transition probabilities, and results in the hypochromicity [45,46]. The interaction of electronic states of the intercalating chromophore with stacked base pairs of DNA causes the contraction of the DNA helix and change in the conformation of DNA. These results suggest that organotin(IV) compounds interact with DNA via the intercalation mode of interaction, since only a hypochromic effect is observed, without any significant change of shifts in the spectral profiles, which is the indication of a weak interaction with DNA [47].

A

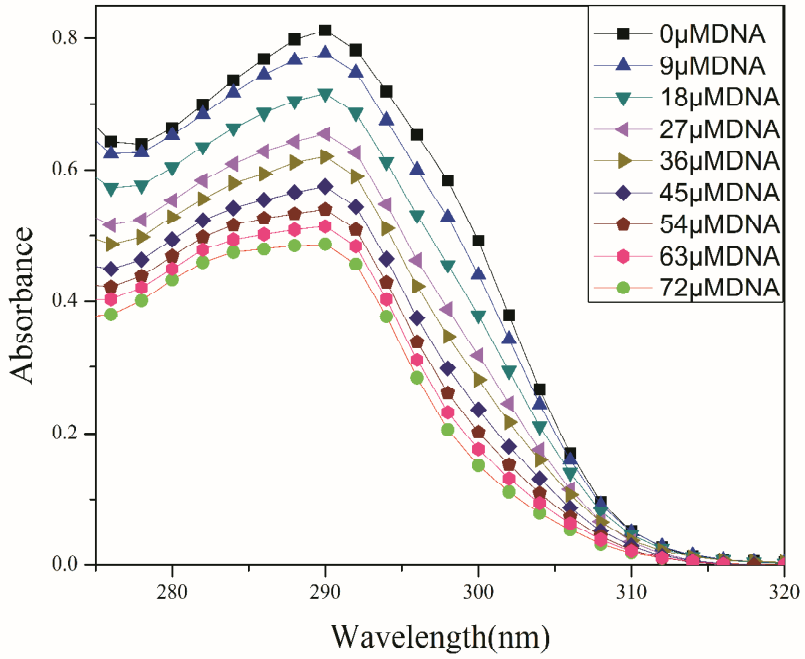

B

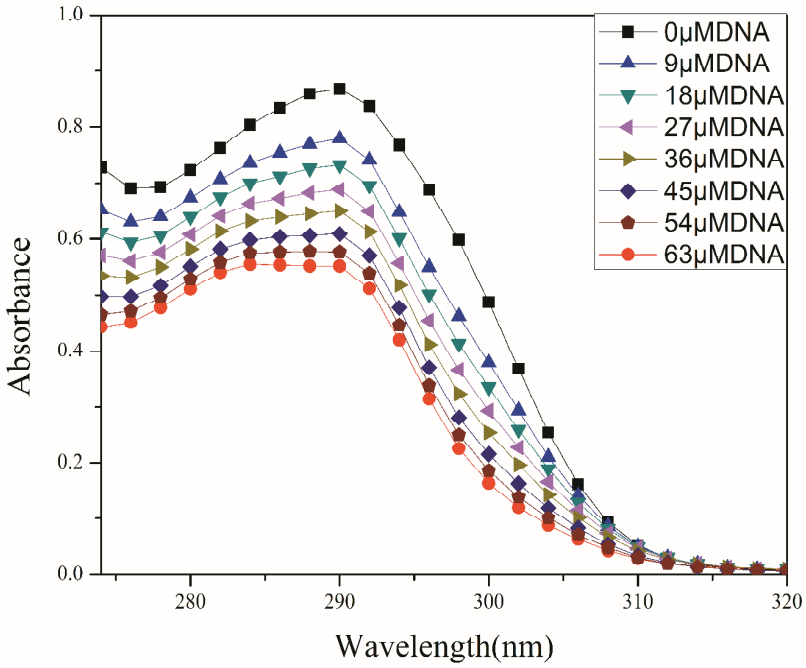

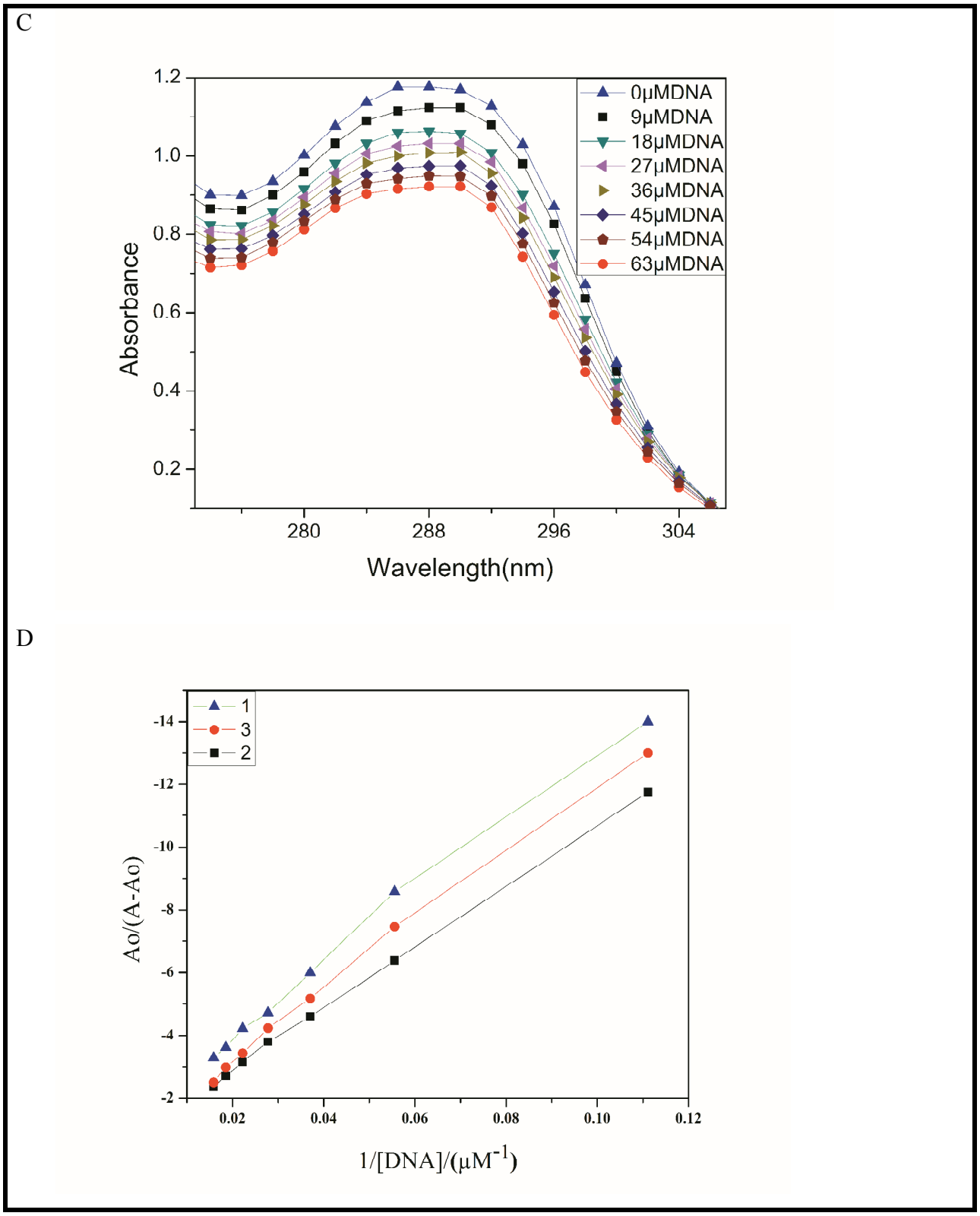

Fig. 4. Absorption spectra of the 2mM compounds (A) Bu_2SnL_2, (B) Me_2SnL_2, (C) Me_3SnL and (D) Plot of Ao/(A-Ao) Vs 1/[DNA] for determination of binding constants for compound 1, 2and 3

The reason for greater association constant of compound**1** is the additional hydrophobic interaction of the butyl groups with bases of DNA [48]. Based upon the variation in absorbance, the association/binding constants of these compounds with DNA were determined according to the Benesi–Hildebrand equation [49];

$$\frac{A_0}{A-A_0}=\frac{\varepsilon_{\mathrm{G}}}{\varepsilon_{\mathrm{H-G}}-\varepsilon_{\mathrm{G}}}+\frac{\varepsilon_{\mathrm{G}}}{\varepsilon_{\mathrm{H-G}}-\varepsilon_{\mathrm{G}}}\times\frac{1}{K[\mathrm{DNA}]}$$

Where K is the binding constant, A_0 and A are the absorbances of the free and DNA bound organotin(IV) compounds

While εG and εH-G are their absorption coefficients respectively.

3.4.2 Compound-DNA interaction study by Viscometery

The change in viscosity of DNA is regulated by the length of DNA, therefore the change in viscosity of DNA upon addition of a compound reflects the intercalative mode of binding. The addition of compound (1-4) to the solution of the DNA results in separation of base pairs to host the binding compound, resulting in the lengthening of the DNA helix and subsequently increased in DNA viscosity as shown Fig.5. On the other hand, the binding of a compound exclusively in DNA grooves by means of partial and/or non-classic intercalation, under the same conditions causes a bend or kink in the DNA helix, reducing its effective length and, as a result, the DNA solution viscosity is decreased or remains unchanged, i.e. groove binders and electrostatic interaction do not increase the lengthen of DNA molecules [50,51]. The present case (Fig.5) suggests an intercalative mode of interaction of the compound (1-4) with DNA.

4. Conclusions

The organotin(IV) derivatives of 3,5-dimethylbenzoic acid ligand exhibit skew-trapezoidal bipyramidal (**1** and **2**) or distorted trigonal bipyramidal coordination geometry (**3**) geometry both in solution and in solid state.

The Gaussia luciferase Assay and real-time PCR assays confirmed the anti-HCV activity of compound **1**. The spectroscopic and viscometery techniques were successfully used for the evaluation of binding parameters of compounds 1–3 with DNA. The UV-titration results agree with the Viscometer data. Based upon the increase in viscosity current and absorption intensity the stability of adduct formation followed the order: 1>3 >2. The results of UV–vis spectra and viscosity indicate that all the compounds 1–3 intercalate into the double helix of DNA. The negative values of ΔG designate the spontaneity of compound–DNA binding. However, further work is required to use compound **1** on a clinical level.

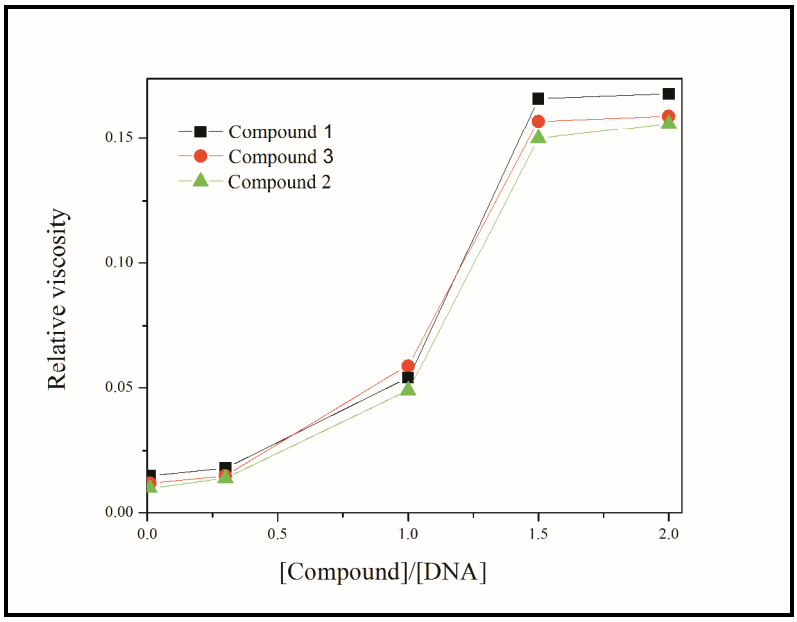

Fig. 5. The relative viscosity of the DNA with the addition of organotin(IV) compounds

5. Supplementary material

CCDC 1003234, 1003233 and 1003235 contain the supplementary crystallographic data for 1, 2 and 3, respectively. These data can be obtained free of charge from The Cambridge Crystallographic Data Centre *via* www.ccdc.cam.ac.uk/data_request/cif.

References

1. WHO. Global burden of diseases (GBD) for hepatitis C. J Clin Pharmacol 44 (1) (2004) 20-9
2. B.J. Thomson, R.G. Finch, Clin. Microbiol. Infect. 11 (2005) 86-94
3. T. Watanabe, T. Umehera, M. Kohara, Adv drug Delivery Rev. 59 (2007) 1263-76
4. M.G. Ghany, D.B. Strader, D.L. Thomas, L.B. Seeff, Hepatology 49(2009) 1335–74
5. European Association for the Study of the Liver. EASL clinical practice guidelines: management of hepatitis C virus infection. J Hepatol 55 (2011) 245–64
6. L. Delang, L. Coelmont, J. Neyts, Viruses-Basel. 2 (2010) 826-866
7. C.M. Lange, C. Sarrazin, S. Zeuzem, Aliment. Pharmacol. Ther. 32 (2010) 14-28
8. R. Flisiak, A. Parfieniuk. Expert. Opin. Investig. Drugs 19 (2010) 63-75
9. A. Opar, Nat. Rev. Drug Disc. 9 (2010) 501-503
10. F.A. Shah, K. Fatima, S. Sabir, S. Ali, I.Qadri, Appl. Organometal. Chem. 28 (2014) 74–80
11. S. Nafisia, A. Sobhanmanesh, M. Esm-Hosseini, K. Alimoghaddamc, H.A.T. Riahid, J. Mol. Struct. 750 (2005) 22–27
12. F.A. Shah, M. Sirajuddin, S. Ali, S.M. Abbas, M.N. Tahir, C. Rizzoli, Inorg Chim Acta. 400 (2013) 159–168
13. D. O'Farrell, R. Trowbridge, D. Rowlands, J. Jager, J. Mol. Biol. 326 (2003) 1025–1035
14. N. Arshad, U. Yunus, S. Razzque, M. Khan, S. Saleem, B. Mirza, N. Rashid, Eur. J. Med. Chem. 47 (2012) 452–461
15. D.M. Tscherne, M.J. Evans, T. von, C.T. Jones, Z. Stamataki, J.A. McKeating, B.D. Lindenbach, C.M. Rice, J. Virol. 81 (2007) 3693-3703

16. B.A. Tannous, D. E. Kim, J. L. Fernandez, R. Weissleder, X.O. Breakefield, Mol. Ther. 11 (2005) 435–443
17. R. Weissleder, V. Ntziachristos, Nat Med. 9 (2003) 123–128
18. P.S. Dittrich, A. Manz, Nat. Rev. Drug Discov. 5 (2006) 210–218
19. M.H. Wu, S.B. Huang, G.B. Lee, Lab Chip. 10 (2010) 939–956
20. W.L.F. Armaergo, C.L.L. Chai, Purification of Laboratory Chemicals, 5th edn. (Butterworth-Heinemann, New York, (2003)
21. *SMART* (Version 5.059), *SAINT-Plus* (Version 6.01) and *SADABS* (Version 2.01). Bruker AXS Inc., Madison, Wisconsin, USA (1998)
22. *APEX-II* (Version 2008.1-0), *SAINT* (Version 7.51A) and *SADABS* (Version 2007/4). Bruker AXS Inc., Madison, Wisconsin, USA (2008)
23. D. Belletti. *FEBO*. Internal Report 1/93, Centro di Studio per la Strutturistica Diffrattometrica del CNR, Parma, Italy (1993)
24. A. C. T. North, D. C. Phillips, F. S. Mathews. Acta Cryst. A24 (1968) 351-359.
25. G. M. Sheldrick. Acta Cryst. A64 (2008) 112
26. A. Altomare, M. C. Burla, M. Camalli, G. Cascarano, C. Giacovazzo, A. Guagliardi, A. G. G. Moliterni, G. Polidori, R. Spagna. J. Appl. Cryst. 32 (1999) 115-119
27. L. J. Farrugia. J. Appl. Cryst. 45 (2012) 849-854
28. E. Keller. *SCHAKAL99*. University of Freiburg, Germany (1999)
29. C. T. Jones, M.T. Catanese, L.M.J. Law, S.R. Khetani, A.J. Syder, A. Ploss, T.S. Oh, J.W. Schoggins, M.R. MacDonald, S.N. Bhatia, C. M. Rice, Nat Biotechnol. 28 (2010) 167–171

30. Y. Zhang, X. Wang, L. Ding, Nucleosides, Nucleotides and Nucleic Acids 30 (2011) 49-62

31. C.V. Sastri, D. Eswaramoorthy, L. Giribabu, B.G. Maiya, J. Inorg. Biochem. 94 (2003) 138-145

32. M. Tariq, N. Muhammad, M. Sirajuddin, S. Ali, N.A. Shah, M.R. Khan, M.N. Tahir, J. Organomet. Chem., 723 (1) (2013) 79-89

33. E.R.T. Tiekink, Trends Organomet. Chem. 1 (1994) 71–116

34. A. Ruzicka, L. Dostal, R. Jambor, V. Buchta, J. Brus, Appl. Organomet. Chem. 16 (2002) 315–322

35. M. Parvez, S. Ali, T. Masood, M. Mazhar, M. Danish, Acta Crystallogr. C53 (1997) 1211-1213

36. C.L. Ma, Q.F. Zhang, R.F. Zhang, L.L. Qiu, J. Organomet. Chem. 690 (2005) 3033-3043

37. A.W. Addison, R.T. Nageswara, J. Reedijk, R.J. Van, G.C. Verschoor, J. Chem. Soc. Dalton Trans. 7 (1984) 1349-1356

38. W. Rehman, A. Badshah, F. Rahim, M.K. Baloch, H. Ullah, O-U-R. Abid, I. Tauseef, Inorganica Chimica Acta. 423 (2014) 177–182

39. S. Marukian, Hepatology. 48 (2008) 1843–1850

40. (a). M. Gielen, R. Willem, Anticancer Res. 12 (1992) 1323-1325 (b). M. Gielen, A. El Khloufi, M. Biesemans, F. Kayser, R. Willem, Appl. Organomet. Chem. 7 (1993) 201-206 (c) M. Gielen, R. Willem, Anticancer Res. 12 (1992) 257-268 (d) D.-S. Zuo, T. Jiang, H.-S. Guan, X. Qi, K.-Q. Wang, Z. Shi, Z. Chin, J. Chem. 19 (2001) 1141-1145

41. F.A. Shah, K. Fatima, S. Sabir, S. Ali, A. Fischer, M.I. Qadri. Med. Chem Res. DOI 10.1007/s00044-014-1242-3

42. A. Bacchi, A. Bonardi, M. Carcelli, P. Mazza, P. Pelagatti, C. Pelizzi, G. Pelizzi, C. Solinas, F. Zani, J. Inorg. Biochem. 69 (1998) 101-112

43. C.Y. Zhou, J. Zhao, Y.B. Wu, C.X. Yin, P. Yang, J. Inorg. Biochem. 101 (2007) 10-18

44. N. Li, Y. Ma, C. Yang, L. Guo, X. Yang, Biophys. Chem. 116 (2005) 199-205

45. C.C. Ju, A.G. Zhang, C.L. Yuan, X.L. Zhao, K.Z. Wang, J. Inorg. Biochem. 105 (2011) 435-443

46. Z. Xu, G. Bai, C. Dong, Bioorg. Med. Chem. 13 (2005) 5694-5699

47. V. Gonzalez-Ruiz, A.I. Olives, M.A. Martin, P. Ribelles, M.T. Ramos, J.C. Menendez, Biomedical Engineering, Trends, Research and Technologies, InTech, India, (2011) 65 (ISBN 978-953-307-514-3)

48. Q. Lie, P. Yang, H. Wang, M. Guo, J. Inorg. Biochem. 64 (1996) 181–195.

49. M.S. Ibrahim, I.S. Shehatta, A.A. Al-nyeli, J. Pharm. Biomed. Anal. 28 (2002) 217-225

50. D. Li, J. Tian, W. Gu, X. Liu, S. Yan, J. Inorg. Biochem. 104 (2010) 171-179

51. M. Jiang, Y. Li, Z. Wu, Z. Liu, C. Yan, J. Inorg. Biochem. 103 (2009) 833-844

Table of Contents

Organotin(IV) based Anti-HCV drugs: Synthesis, Characterization and Biochemical Activity

Farooq Ali Shah[a], Shaista Sabir[b], Kaneez Fatima[c], Saqib Ali[a], Ishtiaq Qadri[d*], Corrado Rizzoli[e]

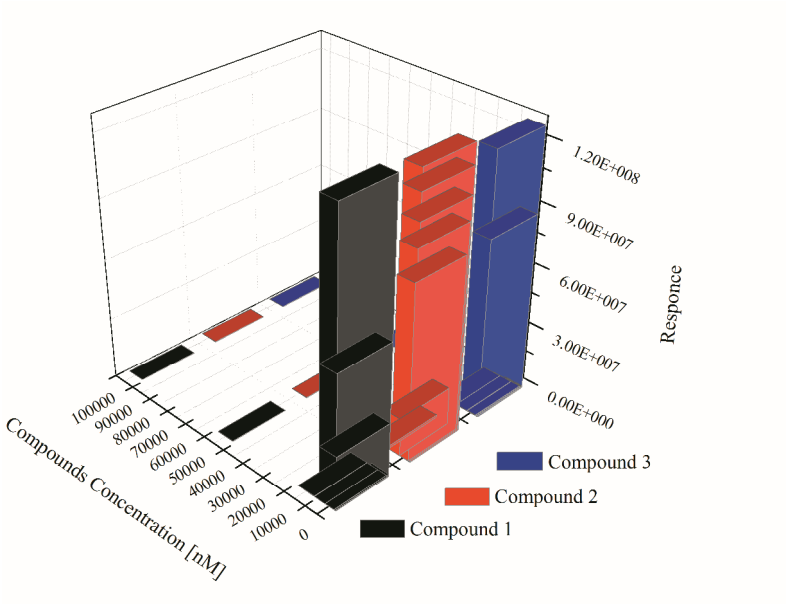

Organotin(IV) compounds are potential anti-HCV agents due to their interaction with RNA and their strong binding constant.

Organotin(IV) based Anti-HCV drugs: Synthesis, Characterization and Biochemical Activity

Farooq Ali Shah[a], Shaista Sabir[b], Kaneez Fatima[c], Saqib Ali[a], Ishtiaq Qadri[d*], Corrado Rizzoli[e]

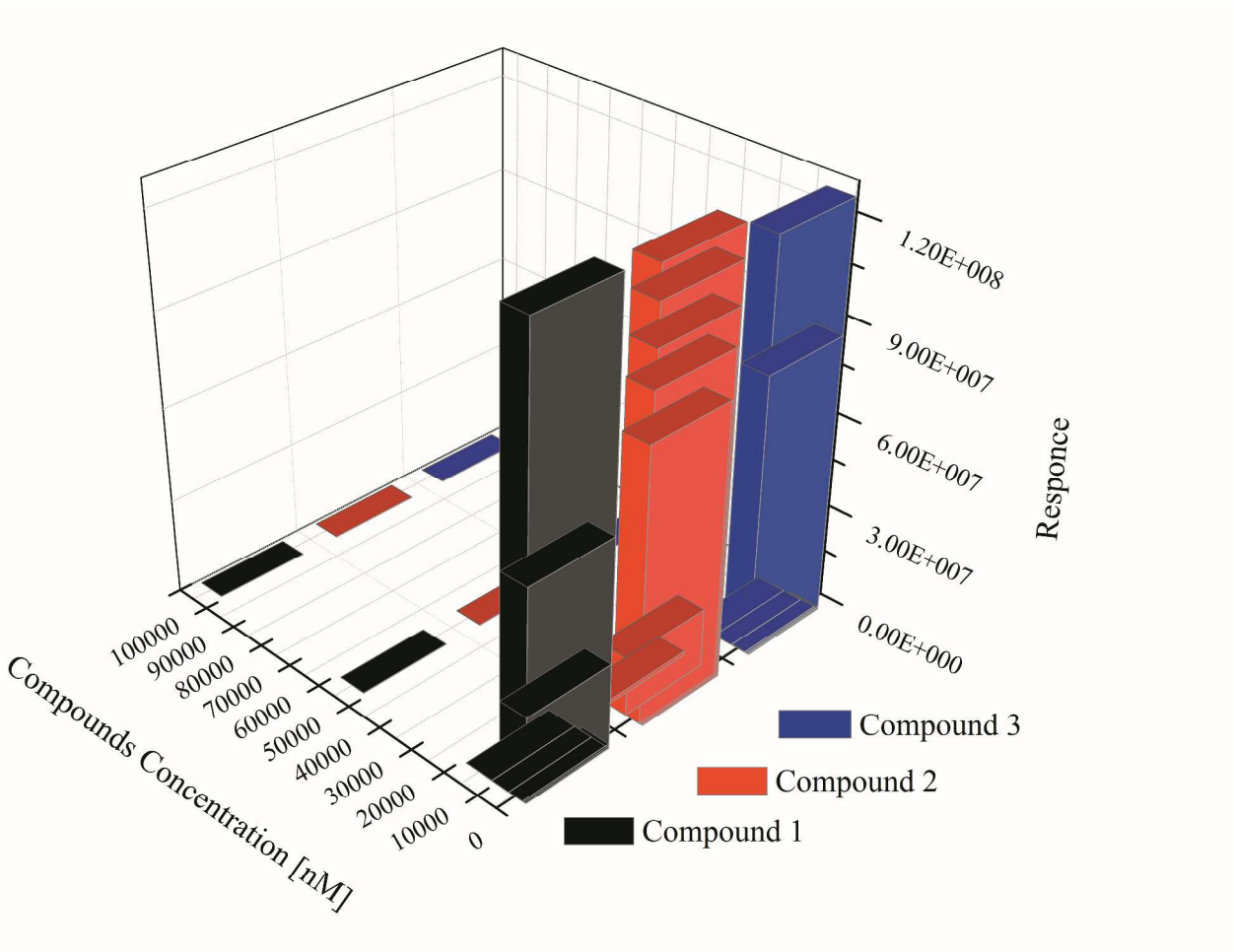

Organotin(IV) compounds are potential anti-HCV agents due to their interaction with RNA and their strong binding constant.